ON THE INCIPIENT FLUIDIZED STATE OF SOLID PARTICLES

Miloslav HARTMAN[a] and Robert W. COUGHLIN[b]

[a] *Institute of Chemical Process Fundamentals, Academy of Sciences of the Czech Republic, 165 02 Prague 6-Suchdol, The Czech Republic*

[b] *Department of Chemical Engineering, University of Connecticut, Storrs, CT 06269, U. S. A.*

Received September 2, 1992
Accepted October 26, 1992

A comprehensive study has been reported on all aspects of the transition of packed bed to the state of incipient fluidization (point of minimum fluidization, onset of fluidization): particle size and shape, size distribution in a batch of particles, fixed bed voidage, pressure drop through a packed bed and onset of fluidization. A number of predictive equations have been compared that were proposed to estimate the minimum fluidization velocity. All the equations tested do not have any flow limitations and are applicable to laminar, transitional as well as to turbulent flow regime. While some equations have some foundation in theory, the other are more or less generalized correlations of experimental data amassed by different authors under various conditions. The influence of temperature and pressure on the minimum fluidization velocity has been explored with respect to the important applications such as combustion and gasification. Problems have also been discussed with transition from fixed to fluidized bed of binary and polydisperse systems.

1. INTRODUCTION

Fluidization has long been recognized as an efficient means of contacting gas and particulate solids. Many chemical reactions are best carried out in fluidized bed reactors which provide excellent temperature control of the reaction volume. The high heat

capacity of the solid particles in combination with the turbulent motion of the bed eliminates or minimizes the formation of hot spots. In general, packed beds are not capable of providing the desired temperature control due to their poorer heat transfer characteristics and the low heat capacities of gases in comparison to heats of reaction. Another advantage of the fluidized state is fluid-like properties that permit easy transport of solids, for example by simple gravity flow.

There are, however, some possible disadvantages of fluidized beds such as excessive entrainment of fines, erosion of bed internals, by-passing of the solids by gas and defluidization. An application of fluidized bed calls for careful design based on the fundamental physics of gas–solid fluidization. Such a fundamental approach would be desirable for reliable scale-up from a smaller reactor to a full-scale operation.

It is known that quantities such as the minimum fluidizing velocity, U_{mf} and the excess gas velocity, $U - U_{mf}$, most markedly affect the behaviour and performance of a fluidized bed, including bubble size, bed expansion and mixing of particles. The state of incipient fluidization is defined here as the condition where the superficial fluid velocity, U, is equal to the minimum fluidizing velocity, U_{mf}. This condition is attained when the particles become just suspended as the velocity of fluid flowing upward through a batch of solids is progressively increased. In other words, the superficial velocity of fluid needed to just fluidize the particles is called the minimum fluidizing velocity.

The incipient fluidized state, which is also called the onset of fluidization, is an important aspect of a fluidized bed and the minimum fluidization velocity is the basic information needed for the design and development of various gas–solid contactors. Although the majority of fluidized bed processes are conducted with polydisperse particles at elevated or high temperature, most research on the basic physical properties of fluidized systems has been done at ambient temperature and pressure with nearly monodisperse materials. In recent years the combustion of low-grade coal, gasification of coal, waste incineration and desulfurization of flue gas has been studied in fluidized beds. Such fluidized systems are operated at elevated or high temperatures (and pressures) and utilize a wide variety of solid particles. The ever increasing commercial use of fluidized operations synchronizes the importance of understanding the influence of temperature and pressure, as well as fluid and particle properties, upon the minimum fluidization velocity and other characteristics of gas-fluidized beds.

While liquid–solid fluidized systems usually expand homogeneously (particulate fluidization, Hartman et al.[1]), gas–solid fluidized systems generally exhibit the formation and flow of non-homogenities (bubbles) through the fluidized beds (aggregative fluidization). The bubbles are usually formed during operation conditions very close to the point of minimum fluidization.

This review paper is linked to our recent work[2] related to predicting the minimum fluidization velocity. In addition, new findings are presented relative to fluidization at

high temperature. A more general treatment of the subject can be found in recent monographs of Yates[3], Levenspiel[4] and Geldart[5].

2. PARTICLE SIZE, SHAPE AND DENSITY

Although it is usual and convenient for researchers to work with approximately monodisperse fractions of spheres, this situation is very rare in engineering practice. Moreover, in practice fundamental parameters such as size, size distribution, shape and density of particles are seldom defined rigorously.

There are several ways of defining the size of a particle of shape other than spherical. The most relevant size parameter for packed and fluidized beds is the surface/volume diameter, d_{sv} (the diameter of a sphere having the same external surface area/volume ratio as the particle).

It can be shown that

$$d_{sv} = \Psi d_v , \qquad (1)$$

where d_v is the volume diameter (the diameter of a sphere having the same volume as the particle). The volume diameter can be computed from the weight and volume of a sample of particles. The volume can be computed from the density or measured by fluid displacement, if the particles are nonporous. The sphericity, Ψ, is the most appropriate single measure for characterizing the shape of irregular and other nonspherical particles. It is defined as

$$\Psi = \left(\frac{\text{surface area of equivalent sphere}}{\text{surface area of the particle}} \right)_{\substack{\text{both of the} \\ \text{same volume}}} \leq 1 . \qquad (2)$$

Thus $\Psi = 1$ for perfect spheres and $0 < \Psi < 1$ for other bodies. The sphericity, and the diameters d_v and d_{sv} can be calculated exactly for geometrical bodies such as spheroids, ellipsoids and other manufactured shapes. The sphericity of irregularly shaped particles can be determined photographically[6] or with the aid of empirically established relations between the sphericity of particles and the voidage of a packed bed of these particles as will be shown below. The sphericities of some geometrically regular bodies as well as those for some other shapes and some common solids are presented in Table I. The values given for the irregular particles should be regarded as estimates only. Viewing particles through a microscope and comparison with the data in Table I will usually provide a realistic value of Ψ.

In most practical situations, particles are irregular and they are generally measured by screen analysis provided that they are larger than about 0.08 mm. The screen size or sieve size, d_p, is then the arithmetic mean of the aperture of the screen which just lets the particles pass through and the next finer screen below on which they are retained.

Unfortunately, there is no general relationship between the screen size, d_p, and the surface/volume diameter, d_{sv}. Abrahamsen and Geldart[7] have attempted to compare the screen size with the volume and surface/volume diameters for crushed quartz. They concluded that for particles which have a sphericity of about 0.8

$$d_v \approx 1.13\, d_p \tag{3}$$

and

$$d_{sv} \approx 0.87\, d_p\,. \tag{4}$$

For spherical or nearly spherical particles, the respective diameters d_{sv}, d_v and d_p agree well. In work with irregularly shaped solids, the surface/volume diameter is usually estimated from the sieve size, d_p, as follows:

$$d_{sv} \approx \Psi\, d_p\,. \tag{5}$$

For a collection of particles of different size, there are several ways of defining an average size. When sieving is used, the mean size, $\bar{d}_p$, directly related to the surface/volume mean can be computed from the individual sieving fractions by

$$\bar{d}_p = 1/\sum (x_i/d_{pi})\,, \tag{6}$$

where the summation is taken over all sieve size fractions, i, and where x_i is the weight fraction of particles in size range i and d_{pi} is the arithmetic average of the adjacent sieve apertures that define size range i.

TABLE I
Sphericities of different shapes, materials and commonly used packings

Particle	Sphericity	Particle	Sphericity
Sphere	1.00	Crushed coal	0.65 – 0.75
Cube	0.81	Crushed particles	0.5 – 0.7
Cylinder, $h = d$	0.87	Pellets	0.7 – 0.8
Cylinder, $h = 5d$	0.70	Wheat	0.85
Sharp sand	0.65	Corn	0.75
Round sand	0.85 – 0.95	Crushed limestone	0.55
Crushed lignite	0.4	Limestone calcine	0.75
Brown coal ash	0.53	Flakes	0.2
Rashig rings	0.26 – 0.53	Corundum	0.82
Berl saddels	0.30 – 0.37		

Another method of characterizing solid particles employs the median, d_{pm}, which is the size corresponding to the 50% value on the cumulative curve of percentage undersize versus sieve aperture. The median, d_{pm}, should not be confused with $\bar{d}_p$ given by Eq. (6). It is apparent that the dispersity within a collected fraction is affected by the differences in the apertures of the adjacent sieves. The Czech Standard series of sieves is arranged in multiples of 1.25, which is close to the British Standard sieve (multiples of 1.189) and U.S. Tyler Standard screen (multiples of 1.189 or 1.414). Since the cumulative curve can conceal some pecularities, weight distribution functions, usually given in the form of a histogram, should be examined to obtain possible additional information.

There is no entirely satisfactory way of comparing the width of the size distribution of different materials, nor of defining how wide a distribution actually is. Geldart[5] recommends to use the relative spread, σ/d_{pm}, in which the spread, σ, is introduced somewhat arbitrarily as

$$\sigma = (d_{84\%} - d_{16\%})/2 . \tag{7}$$

The quantities $d_{84\%}$ and $d_{16\%}$ are read from the cumulative curve and d_{pm} is the median size. Typical values of relative spread range from 0.05 (narrow distribution) through 0.4 (wide distribution) to 0.7 (very wide distribution).

The particle density is defined as

$$\rho_s = M_p/V_p , \tag{8}$$

where M_p is the mass of a single particle and V_p is the particle volume that includes all voids within the particle whether they are open or closed. The particle density is usually determined by mercury or water displacement (pycnometry). Possible causes of some misleading results of pycnometry with small particles ($d_p < 0.15$ mm) have been summarized and discussed by Knight and Rowe[8]. The particle density, ρ_s, should not be confused with the true, skeletal or absolute density of material, ρ_{He}, which is measured by the helium or air pycnometry. The particle density includes the voids or pores in the particle and particle density and absolute density are related to the particle porosity, ε_p, by the relationship

$$\varepsilon_p = 1 - \rho_s/\rho_{He} . \tag{9}$$

3. FIXED BED

3.1. *Bed Voidage*

Fluids passing through a fixed or packed bed of particles flow through passages between the particles. The effective dimensions of the flow passages depend upon the

following variables: porosity (voidage) of the bed, diameter (size) of the particles, sphericity (shape) of the particles, orientation or packing arrangement of the particles and roughness of the particles.

Bed porosity is the most sensitive variable employed in defining a packed bed and should, therefore, be determined with a high degree of accuracy. However, experience shows that high accuracy can be achieved only in very specific situations. For example, the particles adjacent to the wall of a column pack more loosely than the particles in the central part of the bed. It is a well-documented fact that the porosity of bed increases with increasing ratios of particle size to bed diameter[9]. The rougher the particles and column walls, the higher is the void fraction of the bed. For gas–solid systems a satisfactory estimate of the bed porosity can be obtained by pouring a mass W of particles into a cylinder of cross-sectional area F. Then, the values of ε can be calculated from the relation

$$\varepsilon = 1 - W/(FH\rho_s) . \qquad (10)$$

Laboratory experience has shown a significant dependence of height of the poured bed, H, upon the rate of pouring and shaking.

The porosity of a bed is closely related to the sphericity of the particles and also depends upon the size distribution of the particles. The sphericity might be employed as the sole determining factor of bed porosity if the particles were monodisperse, of uniform geometry and everywhere packed in the same spatial arrangements. Unfortunately, those conditions do not hold generally and both the porosity and the sphericity are necessary to define the packed bed. Table II gives experimentally observed values of bed porosity and sphericity for random-packed beds of uniform-sized particles. This

TABLE II
Observed values of the porosity of randomly packed beds as a function of the particle shape[10]

Ψ	ε		Ψ	ε	
	loose packing	dense packing		loose packing	dense packing
0.25	0.85	0.80	0.65	0.55	0.48
0.30	0.80	0.76	0.70	0.53	0.45
0.35	0.75	0.70	0.75	0.51	0.43
0.40	0.72	0.67	0.80	0.48	0.40
0.45	0.67	0.62	0.85	0.47	0.38
0.50	0.64	0.59	0.90	0.45	0.36
0.55	0.60	0.55	0.95	0.43	0.34
0.60	0.58	0.51	1.00	0.42	0.31

table can be used to estimate the particle sphericity provided the bed porosity is known or measured. The voidage of the bed formed by uniformly sized spheres lies in the range $\varepsilon = 0.40$ to 0.42.

It is notable that both the bed voidage and the sphericity of particles employed in defining the bed, are quantities that can be determined for a given real system. In practice, both variables depend upon and are influenced by the experimental techniques used to measure them.

Orientation of the particles is an important factor in some situations. The definition of the mean particle dimension as expressed by Eq. (*6*) is more strongly weighted by fine particles than by larger particles, so small proportions of fine particles can have a disproportionate effect on $\bar{d}_p$. Roughness of the particles is of less importance than the other factors, but may become somewhat more important in highly turbulent flow.

3.2. *Flow and Pressure Drop through a Packed Bed*

For flow through porous media (packed beds), it is desirable to predict the flow rate for a given pressure drop or to predict the pressure drop necessary to achieve a specific flow rate. Although the complexity of flow pattern rules out a rigorous solution of the problem, empirical and semi-empirical solutions exist.

A packed bed can be modelled as a large number of small tortuous pipes or capillaries of varying cross-section. Another approach views the packed bed as an assembly of particles immersed in a fluid. The first approach has proved to be somewhat more practical.

Kozeny[11] combined the Darcy law with the Hagen–Poiseuille equation for laminar flow through straight cylindrical tubes. His expression was later modified by Carman[12] to account for the sinuslike shape of the actual flow paths to give the result:

$$\frac{\Delta P}{H} = 180 \frac{(1-\varepsilon)^2}{\varepsilon^3} \frac{\mu_f U}{(\Psi d_p)^2}, \qquad Re < 1. \tag{11}$$

The Kozeny–Carman equation (*11*) applies at Reynolds numbers less than about 1, Reynolds number being defined in terms of the superficial or empty-column velocity and the particle diameter. Under conditions of laminar flow, the pressure drop is due solely to viscous energy losses. Such conditions occur with beds of particles smaller than about 0.15 mm. There are some indications that the numerical constant in Eq. (*11*) may be accurate only for nearly monodisperse particles, porosities between 0.4 and 0.5, and Reynolds numbers between 0.1 and 1.

In fully developed turbulent flow, the friction factor depends only on the roughness. For such conditions, where the pressure drop is due solely to kinetic energy losses, Burke and Plummer[13] proposed the formula

$$\frac{\Delta P}{H} = 1.75 \frac{1-\varepsilon}{\varepsilon^3} \frac{\rho_f U^2}{\Psi d_p}, \qquad Re > 1\,000. \tag{12}$$

Comparing Eqs (*11*) and (*12*) it can be seen that the viscous energy losses are proportional to $(1 - \varepsilon)^2/\varepsilon^3$ and the kinetic energy losses to $(1 - \varepsilon)/\varepsilon^3$.

3.3. *Model of Ergun*

Seeking to develop a comprehensive formula applicable to all flow regimes, Ergun[14] assumed and verified that the total energy loss in fixed beds can be treated as the sum of viscous and kinetic energy losses. Thus, the Ergun capillary flow model argues that the flow resistance is the sum of a viscous resistance corresponding to the linear term in the relationship

$$\frac{\Delta P}{H} = aU + bU^2 \tag{13}$$

and an inertial resistance corresponding to the quadratic term. The first term on the right-hand side arises from the Kozeny–Carman equation ($Re < 1$) and represents the pressure loss due to skin friction (viscous term). The second term expresses the pressure drop due to form drag (kinetic term) and is given by the Burke–Plummer expression ($Re > 1\,000$). The parameters a and b in Eq. (*13*) are as follows

$$a = 150 \frac{(1-\varepsilon)^2}{\varepsilon^3} \frac{\mu_f}{(\Psi d_p)^2}, \tag{14}$$

$$b = 1.75 \frac{1-\varepsilon}{\varepsilon^3} \frac{\rho_f}{\Psi d_p}. \tag{15}$$

The values of the numerical constants, 150 and 1.75, were computed using more than 600 experimental data points obtained in experiments with various-sized spheres, sand, crushed coke, and the following gases: nitrogen, carbon dioxide, methane and hydrogen.

The Ergun equation is a comprehensive relationship which can be applied to all types of flow. Its predictions are shown in Fig. 1. The Ergun equation has been found to estimate the pressure drop across a fixed bed within an accuracy of ±50%. It should be noted that this equation was developed for ambient temperature and pressure, and for isothermal and incompressible fluids. It also works well for gases when the pressure drop is not high and the gas density is estimated using the mean pressure in the bed. If the pressure drop is high, Eq. (*13*) should be written in differential form and applied

sequentially to small successive increments of ΔP. The structure of the Ergun equation provides a way of estimating the influence of temperature and pressure on the pressure loss of packed beds at various operating conditions.

Under laminar flow conditions ($Re < 1$) the second term on the right-hand side of Eq. (*13*) can be neglected

$$\frac{\Delta P}{H} \sim \frac{\mu_f U}{d_p^2} . \qquad (13a)$$

In fully developed turbulent flow ($Re > 1\,000$) the second term dominates on the right-hand side of Eq. (*13*)

$$\frac{\Delta P}{H} \sim \frac{\rho_f U^2}{d_p} . \qquad (13b)$$

Macdonald et al.[15] and Dullien[16] have tested the Ergun equation using data sets of six researchers for widely different porous media. They found that the specific constant 150 should be replaced by a value of 180 in the viscous flow region. For the inertial flow regime, the numerical parameter is not single-valued, but depends on the particle roughness and lies in the range 1.8 – 4. Their analysis has also suggested that replacing the term ε^3 in the Ergun model with the term $\varepsilon^{3.6}$ would give better results.

It should be mentioned that there are other correlations for predicting the pressure drop in packed beds. For example, Nakamura et al.[17], working at elevated temperatures and pressures, were able to fit their experimental data for fixed beds to the exponential relationship

$$\frac{\Delta P}{H} = C U^n , \qquad (16)$$

where n varied between 1 and 2 as viscous or turbulent forces, respectively, predominated.

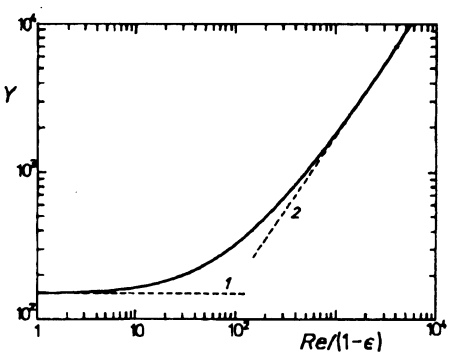

FIG. 1
Graphical representation of the pressure drop in packed columns predicted by the Ergun relationship[14] (full line); asymptotes: *1* Kozeny–Carman, *2* Burke–Plummer

4. ONSET OF FLUIDIZATION

At the condition of minimum fluidization (also called the onset of fluidization) the force exerted by the upward flowing fluid becomes equal to the gravitational force acting on the particles. In other words, the pressure drop across the bed is equal to the apparent weight of the bed particles per unit cross-sectional area of bed as stated by the equation:

$$\left(\frac{\Delta P}{H}\right)_{mf} = (1 - \varepsilon_{mf})(\rho_s - \rho_f) g , \qquad (17)$$

where ε_{mf} is the porosity of bed at minimum fluidization. The porosity ε_{mf} can be estimated by measuring the most loosely packed bulk density of bed. If the bed is composed of interlocked, very angular or cohesive particles, then an excess pressure drop is needed to free them and the equation above refers to the conditions after cohesion or interlocking has been overcome.

4.1. *Ergun Equation*

Equating Eqs (*13*) and (*17*), to eliminate ($\Delta P/H$) results in the quadratic expression

$$(1 - \varepsilon_{mf})(\rho_s - \rho_f) g = 150 \frac{(1 - \varepsilon_{mf})^2}{\varepsilon_{mf}^3} \frac{\mu_f U_{mf}}{(\Psi d_p)^2} + \\ + 1.75 \frac{(1 - \varepsilon_{mf})}{\varepsilon_{mf}^3} \frac{\rho_f U_{mf}^2}{\Psi d_p} . \qquad (18)$$

Equation (*18*) can be rewritten in dimensionless form as

$$\frac{1.75}{\varepsilon_{mf}^3 \Psi} Re_{mf}^2 + \frac{150 (1 - \varepsilon_{mf})}{\varepsilon_{mf}^3 \Psi^2} Re_{mf} - Ar = 0 , \qquad (19)$$

where Ar is the Archimedes number (also called the Galileo number) and Re_{mf} is the Reynolds number at minimum fluidization conditions.

Equation (*19*) can also be written in the form

$$1.75 A Re_{mf}^2 + 150 B Re_{mf} - Ar = 0 , \qquad (20)$$

(kinetic term) (viscous term)

where the parameters A and B are defined functions of void fraction, ε_{mf}, and shape factor, Ψ, only:

$$A = 1/(\varepsilon_{mf}^3 \Psi) \tag{21}$$

and

$$B = (1 - \varepsilon_{mf})/(\varepsilon_{mf}^3 \Psi^2) . \tag{22}$$

Under conditions of laminar flow, where $Re_{mf} < 1$, the minimum fluidization velocity can be predicted from Eq. (*18*) by neglecting the kinetic term:

$$U_{mf} = \frac{1}{150\,B} \frac{d_p^2 (\rho_s - \rho_f) g}{\mu_f} , \qquad Re_{mf} < 1 . \tag{23}$$

In highly turbulent flow, where $Re_{mf} > 1\,000$, the viscous term in Eq. (18) is negligible and we can write

$$U_{mf} = \left(\frac{1}{1.75\,A} \frac{d_p (\rho_s - \rho_f) g}{\rho_f} \right)^{1/2} , \qquad Re_{mf} > 1\,000 . \tag{24}$$

The predictions for U_{mf} given by Eqs (*23*) and (*24*) are significantly different. While the fluid viscosity does not appear in Eq. (*24*), the minimum fluidization velocity changes with the square root of particle size in turbulent flow. The minimum fluidization velocity depends on the square of particle size in the laminar flow regime (Eq. (*23*)). Unlike equations (*23*) and (*24*), Eqs (*18*) – (*20*) have no flow restrictions and are applicable in both the laminar and the turbulent flow regime. It should be noted that the predictions of the minimum fluidization velocity provided by the Ergun equation are very sensitive to the minimum fluidization bed voidage. In the laminar flow regime an error of 3% in the estimate of ε_{mf} leads to an error of about 11% in predicted U_{mf}.

The state of incipient fluidization has been traditionally determined by noting the flow rate at which the pressure drop stops increasing with increasing fluid velocity, and remains essentially constant thereafter. Useful experimental details on this technique can be found elsewhere[2]. This conventional or macroscopic method has been supplemented with an instrumental technique which determines the minimum fluidization velocity by microscopic or stochastic measurements[2,18 - 20]. This newer approach determines the onset of fluidization as the condition where significant rapid pressure fluctuations begin. A sensitive pressure probe placed immediately above the distributor detects a fluctuating pressure signal from any point in the bed. The pressure fluctuations reflect directly the dynamic nature of a fluidized bed. This instrumental technique is particularly useful in measuring the incipient fluidization in a bed of complex confi-

guration wherein the starting point of fluidization is not distinct as, for example, in tapered (conical) beds[21 - 23].

In this dynamic method, the onset of fluidization is indicated when the pressure drop signal abruptly starts to fluctuate rapidly as illustrated in Fig. 2.

4.2. *Equation of Wen and Yu*

Another theoretical formulation for incipient fluidization of spherical particles is based on a steady-state balance of forces acting on an individual solid particle in the fluidized bed[24 - 29]. The drag force is set equal to the difference between the gravitational and buoyancy forces according to the equation:

$$\frac{\pi d_p^3}{6} (\rho_s - \rho_f) g = f(\varepsilon) \left(C_D \frac{\rho_f U^2}{2} \frac{\pi d_p^2}{4} \right), \tag{25}$$

where

$$f(\varepsilon) = F_{DA}/F_{Di} \tag{26}$$

is the ratio of drag forces acting on a particle in the assembly of particles (F_{DA}) and on an isolated particle (F_{Di}).

Under conditions of incipient fluidization, Eq. (25) can be rearranged to

$$\frac{3}{4} f(\varepsilon_{mf}) C_D Re_{mf}^2 = Ar, \tag{27}$$

where $C_D = C_D (Re_{mf})$.

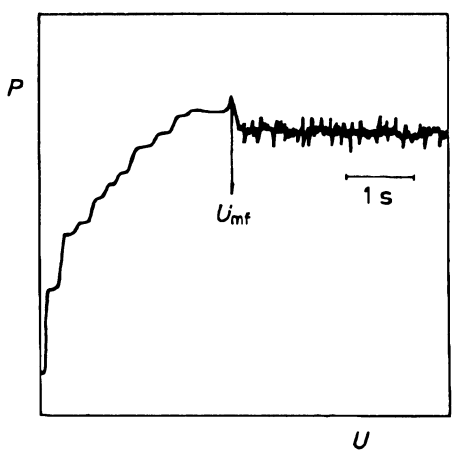

FIG. 2
Detection of the state of incipient fluidization by a sensitive pressure probe[20]

For the terminal free fall velocity of a single sphere in a uniform infinite medium[28,29], the Eq. (*27*) reduces to

$$C_D Re_t^2 = \frac{4}{3} Ar , \qquad [\varepsilon = 1, Re_t] , \tag{28}$$

where $f(\varepsilon_{mf})$ has been set equal to unity according to Eq. (*26*) for a single particle.

Wen and Yu[24] employed the widely accepted empirical expression of Schiller and Neumann[30] for the drag coefficient of a sphere

$$C_D = 24 (1 + 0.15 Re^{0.687}) / Re \tag{29}$$

which is valid over the range $0.1 < Re < 500 - 1\,000$. As the voidage function $f(\varepsilon_{mf})$, Wen and Yu[24] proposed the empirical relationship

$$f(\varepsilon_{mf}) = 1/\varepsilon_{mf}^{4.7} . \tag{30}$$

Using these last two relations Eq. (*27*) can be rewritten as

$$2.7 Re_{mf}^{1.687} + 18 Re_{mf} - \varepsilon^{4.7} Ar = 0 , \qquad \Psi = 1 . \tag{31}$$

Equation (*31*) can easily be solved for Re_{mf} by an elementary technique such as the interval halving. Introducting the shape factor and keeping the original form of Re_{mf} and Ar provides the Wen–Yu equation for nonspherical particles:

$$2.7 \Psi^{0.687} Re_{mf}^{1.687} + 18 Re_{mf} - \Psi^2 \varepsilon^{4.7} Ar = 0 . \tag{32}$$

The foregoing development by Wen and Yu[24] predicts that the minimum fluidization velocity is very sensitive to the bed voidage. In the laminar flow regime, an error of 3% in the estimate of ε_{mf} leads to an error of 14% in the prediction of U_{mf}.

Values of the Reynolds number, Re_{mf}, at minimum fluidization velocity as predicted by the Ergun equation (*19*) and the Wen and Yu equation (*32*) are compared in Table III. As evident there are appreciable differencies in Re_{mf} which range between –25 and +28% for Archimedes number values ranging from 1 through 10^8.

4.3. *Simplified Empirical Equations*

Both bed voidage, ε_{mf}, and sphericity, Ψ, employed in the predictive expressions are often determined only imperfectly for a given real system. In practice, both factors are not independent and are influenced by the experimental measurement techniques as

well. When no information on Ψ and ε_{mf} is available for a given material, the values presented in Tables I and II can be employed as useful estimates.

In order to avoid the difficulties and uncertainties accompanying the estimation of Ψ and ε_{mf}, Wen and Yu[31] proposed a simplified method for predicting the minimum fluidizing velocity. On the basis of almost three hundred experimental measurements found in the literature, these authors[31] approximated the sphericity-voidage functions A and B (Eqs (*21*) and (*22*)) by the constants

$$A \approx 14 \quad \text{and} \quad B \approx 11 . \tag{33}$$

Then the predictive correlation becomes

$$Re_{mf} = [(33.67)^2 + 0.04082\, Ar]^{1/2} - 33.67 . \tag{34}$$

The simple correlation embodied in Eq. (*34*) covers the wide Re_{mf} range, from 0.001 to 4 000, and predicts Re_{mf} with an overall standard deviation of ±34%. This method makes it possible to circumvent the need to determine Ψ and ε_{mf}. On the other hand such simplification can result in a significant loss of accuracy.

Many researchers have followed the approach of Wen and Yu[31] and fitted their experimental measurements of the minimum fluidization velocity to an empirical function of the form

$$Re_{mf} = (C_1^2 + C_2 Ar)^{1/2} - C_1 . \tag{35}$$

TABLE III
Values of Reynolds number at minimum fluidization predicted by the equations of Ergun[14] and Wen and Yu[31] for spheres (Ψ = 1, ε_{mf} = 0.41)

Ar	Re_{mf}		δ, %
	Ergun, Eq. (*19*)	Wen and Yu, Eq. (*32*)	
1	0.000778	0.000840	−7.6
10	0.007786	0.008363	−7.2
10^2	0.07776	0.08190	−5.2
10^3	0.7671	0.7489	2.4
10^4	6.858	5.637	19.6
10^5	42.37	32.05	27.7
10^6	174.8	148.6	16.2
10^7	602.8	623.8	−3.4
10^8	1 959.0	2 511.0	−24.7

The constants C_1 and C_2 are usually computed by a simple optimization technique. It is apparent that computed values of these constants always depend on the nature of the solids and fluids used in the experiments. As can be seen in Table IV, considerably different constants have been reported in the literature for various materials.

Comparing the empirical equation (*35*) with the original Ergun equations (*19*) and (*22*) indicates that the parameters C_1 and C_2 depend on the porosity, ε_{mf}, and the sphericity, Ψ, as follows:

$$C_1 = 42.86\,(1 - \varepsilon_{mf})/\Psi = 42.86\,B/A \qquad (36)$$

$$C_2 = \Psi\,\varepsilon_{mf}^3/1.75 = 1/(1.75A)\,. \qquad (37)$$

As shown in Table II, the bed voidage decreases monotonically as the particle sphericity increases. Making use of this behaviour Lucas et al.[35,36] classified particulate materials into three categories of decreasing sphericity: round particles, sharp particles and least spherical particles. They analyzed a large amount of data from different sources covering a wide range of values of d_p, Ψ, ε_{mf} and different fluidizing media to determine values of C_1 and C_2 in Eq. (*35*) in each of the three defined sphericity ranges with the following results:

For round particles ($0.8 < \Psi < 1$):

$$Re_{mf} = (870.25 + 0.0357\,Ar)^{1/2} - 29.5\,. \qquad (38)$$

TABLE IV
Shape-voidage functions A and B in Eq. (*20*) and the constants C_1 and C_2 in Eq. (*35*)

Reference	A	B	C_1	C_2
Nakamura at al.[17]	12.3	9.73	33.95	0.0465
Wen and Yu[31]	14	11	33.67	0.04082
Saxena and Vogel[32]	10	5.9	25.28	0.0571
Grace[33]	14	8.89	27.2	0.0408
Chitester et al.[34]	11.6	7.75	28.7	0.0494
Lucas et al.[35,36]	16	11	29.5	0.0357
	nearly spherical particles: $0.8 < \Psi < 1$			
	10	7.5	32.1	0.0571
	sharp particles: $0.5 < \Psi < 0.8$			
	8.5	5	25.2	0.0672
	least spherical particles: $0.1 < \Psi < 0.5$			
Kocurek and Hartman[37]	20.2	10	21.3	0.0283

Equation (*38*) is based on 107 data points correlated with an average standard deviation of Re_{mf} of ±21%.

For sharp particles ($0.5 < \Psi < 0.8$):

$$Re_{mf} = (1\,030.4 + 0.0571\,Ar)^{1/2} - 32.1 . \qquad (39)$$

Equation (*39*) is based on 24 data points correlated with an average standard deviation of Re_{mf} of ±23%.

For particles of lowest sphericity ($0.1 < \Psi < 0.5$):

$$Re_{mf} = (635.0 + 0.0672\,Ar)^{1/2} - 25.2 . \qquad (40)$$

Equation (*40*) is based on only 6 data points correlated with an average standard deviation of Re_{mf} of ±22%.

Broadhurst and Becker[6] followed another approach to develop a generalized equation for estimating U_{mf}, in which sphericity and void fraction do not appear. These authors conducted experiments with a variety of materials over wide ranges of column diameter, bed depth, particle diameter, particle density, and gas properties. Using the theory of dimensionless groups, the correlation equation

$$Re_{mf} = \left(\frac{Ar^{1.85}}{2.42 . 10^5 (\rho_s/\rho_f)^{0.13} + 37.7\,Ar^{0.85}} \right)^{1/2} \qquad (41)$$

was developed with the aid of statistical techniques. For wide ranges of parameters ($10^{-2} < Re_{mf} < 10^3$ and $5 . 10^2 < \rho_s/\rho_f < 5 . 10^4$), Eq. (*41*) predicts the minimum fluidizing velocity within ±37%. Although the correlation (*41*) should preferably be used for regular particles of higher sphericities ($\Psi > 0.8$), we have used this equation to obtain satisfactory agreement between experimental and predicted values of U_{mf} for irregular, flake-like particles of low sphericity[38].

Another empirical correlation, without Ψ and ε_{mf}, that is commonly employed in the non-English literature, is the relationship developed by Goroshko et al.[39]

$$Re_{mf} = \frac{Ar}{1\,400 + 5.22\,Ar^{1/2}} \qquad (42)$$

for spherical particles ($\varepsilon_{mf} = 0.4$).

Table V compares predictions of three generalized equations (*34*), (*38*) and (*41*). The predictions appear to be in reasonably good agreement, especially those provided by these three correlations are close in the middle ranges of Re_{mf} and Ar. These relationships need no knowledge of the particle sphericity or the bed voidage. They are not

subject to any specific flow limitations and can be applied to any practical conditions of flow. However, they should not be used when ε_{mf} and Ψ are known. If ε_{mf} and Ψ are known, the original Ergun equation (*19*) or the Wen–Yu equation (*32*) give better estimates of U_{mf} than their simplified versions. Unfortunately, in most instances reliable quantitative information as to ε_{mf} and Ψ is not available. Tables I and II permit useful estimates of the likely ranges of ε_{mf} and Ψ for many practical situations.

4.4. *Influence of Temperature*

Most fluidized bed processes are conducted at elevated temperatures and pressures whereas almost all research on the fundamental behaviour of fluidized systems has been done at ambient conditions. Although changes in particle size, shape, and density due to increased temperature can usually be neglected, important phenomena as chemical reactions, softening, sticking or agglomeration of particles can occur at elevated temperatures.

The fluidization behaviour of any particulate material is strongly influenced by the physical properties of the fluidizing fluid. The effect of temperature and pressure on the density of gas can be approximated by the equation of state of an ideal gas

$$\rho_g = 0.1203\,MP/T \qquad (43)$$

$$\rho_{air} = 3.489\,P/T\,. \qquad (44)$$

TABLE V
Values of Reynolds number at minimum fluidization estimated by the generalized empirical correlations of Wen and Yu (Eq. (*34*)), Lucas et al. (Eq. (*38*)), and Broadhurst and Becker (Eq. (*41*))

Ar	Re_{mf}			δ, %		
	Eq.(*34*)	Eq.(*38*)	Eq.(*41*)	Eq.(*34*)	Eq.(*38*)	Eq.(*41*)
10	0.00605	0.00605	0.0103	−19.0	−19.0	37.9
10^2	0.0605	0.0604	0.0872	−12.8	−12.9	25.7
10^3	0.600	0.599	0.728	−6.6	−6.7	13.3
10^4	5.59	5.53	5.78	−0.8	−1.8	2.6
10^5	38.52	37.13	36.60	2.9	0.8	−2.2
10^6	171.1	161.7	152.6	5.7	−0.1	−5.7
10^7	609.9	568.7	510.1	8.4	1.0	−9.4
10^8	1 986.0	1 860.0	1 626.0	8.9	2.0	−10.8

Gas viscosity depends only weakly on pressure but increases markedly with temperature as described by the following empirical equations:

$$\mu_{\text{nitrogen}} = 1.5 \cdot 10^{-6} \frac{T^{1.5}}{123.6 + T} \tag{45}$$

$$\mu_{\text{air}} = 1.81 \cdot 10^{-5} \left(\frac{T}{293}\right)^{0.66} . \tag{46}$$

Assuming neither the voidage at minimum fluidization nor the size and shape of particles depend on temperature, the effect of operating temperature on U_{mf} can be assessed using the Ergun equation. The quadratic structure of Ergun's equation (*13*) suggests that U_{mf} is not, in general, a linear function of T. In laminar flow ($Re_{\text{mf}} < 1$), where the viscous loss and only the first term on the right-hand side of Eq. (*13*) dominates, the minimum fluidization velocity is inversely proportional to the gas viscosity

$$U_{\text{mf}} \sim 1/\mu_{\text{g}} , \qquad Re_{\text{mf}} < 1 . \tag{47}$$

Because gas viscosity increases with increase in temperature, U_{mf} decreases with temperature for small Reynolds numbers (small particles):

$$U_{\text{mf}} \sim T^{-0.6} \quad \text{to} \quad T^{-1} , \qquad Re_{\text{mf}} < 1 . \tag{48}$$

For turbulent flow ($Re_{\text{mf}} > 1\,000$), where the kinetic loss i.e., the second term on the right-hand side of Eq. (*13*) predominates, the minimum fluidizing velocity is inversely proportional to the square root of the gas density:

$$U_{\text{mf}} \sim (1/\rho_{\text{g}})^{0.5} , \qquad Re_{\text{mf}} > 1\,000 . \tag{49}$$

The density of a gas decreases as its temperature increases so that U_{mf} increases with temperature at large Reynolds numbers according to the expression

$$U_{\text{mf}} \sim T^{0.5} , \qquad Re_{\text{mf}} > 1\,000 . \tag{50}$$

In the transition regime of flow conditions ($1 < Re_{\text{mf}} < 1\,000$), U_{mf} is proportional to the absolute temperature raised to a power ranging from -1 to $+0.5$:

$$U_{\text{mf}} \sim T^{-1} \quad \text{to} \quad T^{0.5} , \qquad 1 < Re_{\text{mf}} < 1\,000 . \tag{51}$$

As will be shown in the following paragraphs, the velocity of minimum fluidization is essentially independent of temperature under conditions when $Re_{\text{mf}} \approx 37 - 47$, i.e.,

$$U_{mf} \sim T^0, \qquad Re = 37 - 47. \tag{52}$$

In previous publications[38,40,41] we explored the influence of temperature on the state of incipient fluidization of lime particles used for sulfur removal in a fluidized bed reactor. In that work we employed the following Modified Ergun (ME) equation:

$$\frac{k_1}{\varepsilon_{mf}^3} Re_{mf}^2 + \frac{k_2 (1 - \varepsilon_{mf})}{\varepsilon_{mf}^3 \Psi^2} Re_{mf} - Ar = 0, \tag{53}$$

wherein the constants 1.75 and 150 in the original Ergun equation are replaced by the more general coefficients k_1 and k_2. These coefficients were determined by numerical treatment of the experimental data for U_{mf} of lime particles (d_p = 0.565 mm – 1.22 mm) in the temperature range between 20 and 870 °C. The mean bed voidage, ε_{mf}, and the particle sphericity of lime, Ψ, were found to be as large as 0.51 and 0.69, respectively. The viscous term constant k_2 varied from 140 to 150 and did not show any dependence on temperature. The kinetic term constant k_1 was found to increase quite rapidly with temperature as described by a linear empirical equation

$$k_1 = 1.053 + 6.503 \cdot 10^{-3} T. \tag{54}$$

Using ε_{mf} = 0.51, Ψ = 0.69 and k_2 = 145, the minimum fluidization velocities of several lime fractions are predicted by the ME equation (*53*) and Eq. (*54*) with accuracy better than 7.5%. Of course, the semiempirical ME correlation has the usual limitations and should be applied with caution outside the experimental conditions from which it was deduced.

As follows from the equations above, the dependence of U_{mf} on temperature arises from the effect of temperature on the Reynolds number, Re_{mf}, the fluid viscosity, and the fluid density. In general, the minimum fluidization velocity is a nonlinear function of temperature which can exhibit a maximum.

In Fig. 3, predictions of the ME equations (*53*) and (*54*), the Wen–Yu (W–Y) equation (*34*) and the Broadhurst–Becker (B–B) correlation (*41*) are compared regarding influence of temperature on U_{mf}. It is evident that the W–Y equation predicts the largest sensitivity to temperature. Compared with the predictions of the ME equation, the W–Y equation tends to overstate the influence of temperature upon the minimum fluidization velocity. It should be noted that both the B–B and W–Y equations were deduced from experimental measurements conducted at ambient temperature.

Experimental data for the flow regime in which the kinetic losses are important or dominant were reported by Pattipati and Wen[42], Botterill et al.[43] and Flamant et al.[44]. Using large particles of sand (d_p = 3.4 mm), Pattipati and Wen[42] found a steady increase in U_{mf} from 1.55 to 2.12 m s^{-1} with increasing temperature in the range 45 – 505 °C.

The opposite trend was reported by Flamant et al.[44] for corundum particles smaller than 0.6 mm at temperatures ranging from 20 to 900 °C.

The structure of the Ergun equation hints at the existence of a maximum in the function $U_{mf} = U_{mf}(T)$. The experimental data of Botterill et al.[43] plotted in Fig. 4 also suggest such a maximum might occur. The W–Y and B–B computed curves also exhibit feeble maximums at 505 and 485 °C, respectively, for Botterill's particles of sand (d_p = 2.3 mm). Though different approaches were employed to develop these two equations, their predictions are in fair agreement.

As the particle size and/or density increase, the maximum on the curve $U_{mf} = U_{mf}(T)$ moves towards higher temperatures as shown by results systematically computed from the B–B correlation and plotted in Fig. 5 where the solid lines define conditions under which maximum U_{mf} occurs. Systematic computations also show other interesting results. Computations using the W–Y equation indicate that $(dU_{mf}/dT) = 0$ at $Re_{mf} \approx 44$ independent of the sizes or densities of the particles. Computations with the B–B equation, however, indicate that the Reynolds number at which the maximum occurs increases moderately with increasing particle size and particle density as shown in Fig. 6 where the range of Re_{mf} covers the values from 37 to 47. It is interesting to note that the flat maximum occurs on the experimental curve $U_{mf} = U_{mf}(T)$ at Re_{mf} = 49 (U_{mf} = 1.7 m s^{-1}, 400 °C, d_p = 1.7 mm, ρ_s = 3 950 kg m^{-3}) as reported by Flamant et al.[44].

In practice, the condition of minimum fluidization at a temperature of interest is often predicted from measurements at room temperature. The above results indicate

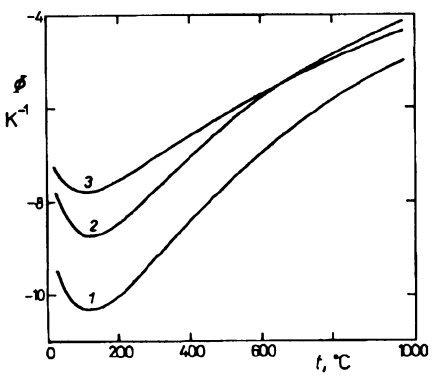

FIG. 3

Influence of temperature on $\Phi \equiv (dU_{mf}/dT)/U_{mf}$ for lime particles fluidized with air[41], particle size d_p = 0.9 mm: *1* Wen–Yu equation (*3.1*), *2* Broadhurst–Becker equation (*4.1*), *3* Modified Ergun equations (*5.3*) and (*5.4*)

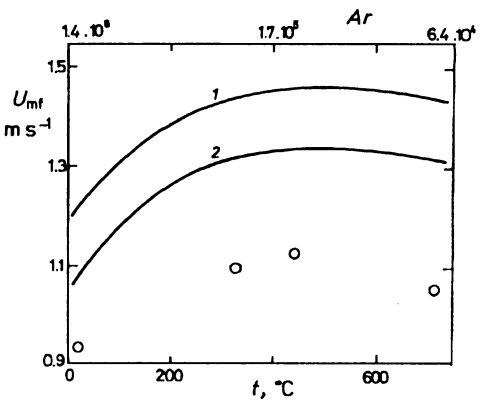

FIG. 4

Dependence of the minimum fluidization velocity on temperature[41]: ○Experimental data of Botterill et al.[43], $\bar{d}_p$ = 2.3 mm (size range: 1.6 – 3 mm), Re_{mf} = 21.6 – 144; *1* prediction of the W–Y equation (*3.1*), *2* prediction of the B–B equation (*4.1*)

that this should be done with caution using generalized correlations such as the Ergun, B–B or W–Y equation.

Other experimental reports[45 - 55] on the behaviour of high temperature fluidized beds indicate that measured U_{mf} decreases with increasing operating temperature for beds of smaller particle size as expected. For example, U_{mf} of sand particles (ρ_s = 2 540 kg m^{-3}) as large as 0.89 mm decreases from 0.43 m s^{-1} at 25 °C to 0.31 m s^{-1} at 620 °C. When the flow is turbulent/transitional with larger particles, gas density becomes the dominant factor and U_{mf} then increases with increasing temperature. For corundum particles (ρ_s = 3 950 kg m^{-3}) having d_p = 2.36 mm, it was reported[44] that U_{mf} increases from 1.75 m s^{-1} to 2.3 m s^{-1} as temperature increases from 20 °C to 700 °C.

Comparing measured and estimated values of U_{mf} suggests that the B–B, W–Y and Ergun equations predict that the incipient fluidization velocity will fall more steeply with increasing temperature than is actually observed experimentally. Because the physical properties of gases can be accurately predicted at the operating temperature and the solids density is essentially independent of temperature, it appears that the real cause of the disagreement between experiment and predictions may lie in the structure of the bed at minimum fluidization.

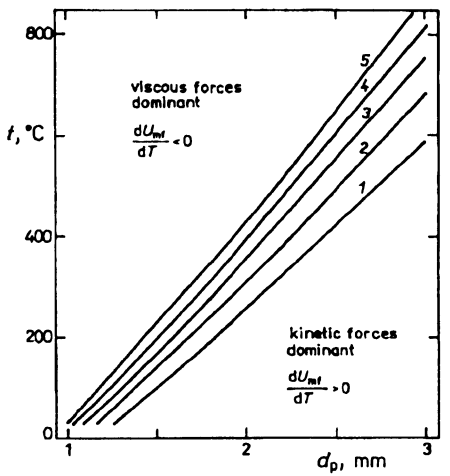

FIG. 5

Influence of particle size and particle density on the temperature at which the function $U_{mf} = U_{mf}(T)$ exhibits the maximum, $(dU_{mf}/dT) = 0$. The lines show the values predicted by the B–B equation (*41*) for fluidization with air: *1* ρ_s = 1 500 kg m^{-3}, *2* ρ_s = 2 000 kg m^{-3}, *3* ρ_s = 2 500 kg m^{-3}, *4* ρ_s = 3 000 kg m^{-3}, *5* ρ_s = 3 500 kg m^{-3}

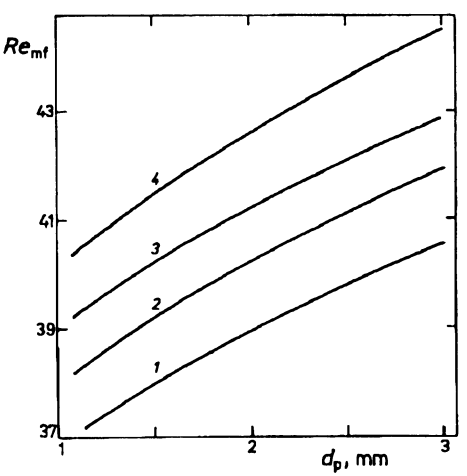

FIG. 6

Influence of particle size and particle density on the Reynolds number at which the function $U = U_{mf}(T)$ exhibits the maximum, $(dU_{mf}/dT) = 0$. The lines represent the values predicted by the B–B equation (*41*) for fluidization with air: *1* ρ_s = 1 500 kg m^{-3}, *2* ρ_s = 2 000 kg m^{-3}, *3* ρ_s = 2 500 kg m^{-3}, *4* ρ_s = 3 500 kg m^{-3}

Botterill et al.[43] determined the average bed voidage at elevated temperatures from measured pressure drop

$$\varepsilon = 1 - \frac{1}{(\rho_s - \rho_g)\, g} \frac{\Delta P}{\Delta H} \tag{55}$$

at different $U > U_{mf}$ and extrapolated to $U = U_{mf}$ to obtain values of ε_{mf} that increased with increasing temperature for small particles. Independent measurements of bed height under conditions near incipient fluidization also showed a slight increase of the bed voidage with increasing temperature[38,53]. In this latter method, ε_{mf} was computed from measured heights of a bed according to the conservation relationship

$$H_0/H_{mf} = (1 - \varepsilon_{mf})/(1 - \varepsilon_0)\,, \tag{56}$$

where H_0 and ε_0 are the height and porosity of the fixed bed[56].

The influence of temperature on the minimum fluidization voidage has not yet been established unambiguously. For example, Pattipati and Wen[42] have reported that ε_{mf} is independent of temperature whereas Botterill et al.[43], Lucas et al.[54] and Saxena et al.[55] found that ε_{mf} depends on the bed temperature. Some experimental measurements of ε_{mf} for larger particles of silica sand are plotted in Fig. 7. As shown by this figure, the results of Botterill et al.[43] and Saxena et al.[55] are considerably different even for very similar particles. Changes in ε_{mf} may occur due to changes in interparticle forces as the flow field around the particles is influenced by changes in temperature, Re_{mf} or Ar. Our experimental evidence indicates that the minimum fluidization voidage increases weakly with temperature for particles smaller than 0.6 mm.

With respect to possible dependence of ε_{mf} on temperatures, theory predicts that the onset of fluidization depends strongly on the bed voidage. Although ε_{mf} is a simple

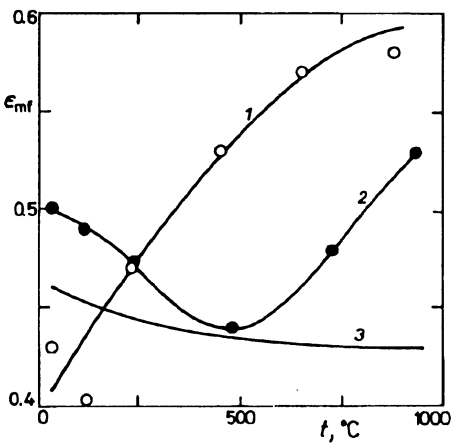

FIG. 7
Variation in the minimum fluidization voidage with increasing bed temperature for beds composed of sand particles of different size and sphericity: *1* observations of Saxena et al.[55] for d_p = 0.75 mm, Ψ = 0.73; *2* observations of Saxena et al.[55] for d_p = 1.22 mm, Ψ = 0.8; *3* observations of Botterill et al.[43] for d_p = 1.28 mm, Ψ = 0.74

concept, its value is particularly difficult to measure at high temperatures and, therefore, susceptible to experimental error. It seems likely that changes in ε_{mf} with temperature are small.

The foregoing discussion pertains only to normal fluidization when neither particle softening nor agglomeration occur. Sintering or agglomeration can occur, however, at temperatures approaching softening points, at high moisture contents[57] or when chemical reactions occur. Fine particles are more susceptible to agglomeration than larger particles. Working with lignite ash (d_p = 0.9 mm) we detected[38] the onset of agglomerating at 600 °C. Under circumstances of agglomeration of particles predictions of U_{mf} are almost futile.

4.5. *Influence of Pressure*

Gas viscosity is essentially independent of pressure up to approximately 3 MPa. Since $\rho_s >> \rho_g$, it follows from Eq. (*23*) that U_{mf} is also virtually independent of pressure in the laminar flow regime where $Re_{mf} < 1$, i.e., for particles smaller than about 0.1 mm.

In turbulent flow, the Ergun equation (*24*) indicates that U_{mf} decreases with increasing gas density or pressure according to the relations

$$U_{mf} \sim \rho_g^{-1/2}, \qquad Re_{mf} > 1\,000 \tag{57}$$

and then

$$U_{mf} \sim P^{-1/2}, \qquad Re_{mf} > 1\,000\,. \tag{58}$$

In the transition flow region ($1 < Re_{mf} < 1\,000$), the minimum fluidization velocity is proportional to pressure raised to a power between 0 and −1/2:

$$U_{mf} \sim P^{0} \quad \text{to} \quad P^{-1/2}, \qquad 1 < Re_{mf} < 1\,000\,. \tag{59}$$

Experimental findings for U_{mf} are in general agreement with the theory[58 - 63]. For beds of larger particles, the minimum fluidization velocity decreases with increasing pressure. The effect of pressure on U_{mf} is more pronounced for heavier particles and is well described by the Ergun equation.

Experimental information thus far available does not permit an unequivocal conclusion as to the influence of pressure on bed voidage at incipient fluidization. In some instances ε_{mf} has been observed to be independent of pressure. Other reports indicate a slight increase of ε_{mf} with increasing pressure as illustrated in Fig. 8.

4.6. *Binary and Polydisperse Mixtures of Particles*

All the experiments discussed above were performed with more or less narrow size fractions of various particles. However, virtually all practical applications involve multicomponent or polydisperse fluidized beds. Combustion, gasification and drying of solids are operations in which multicomponent beds are actually used in practice. The possible combinations of particle size, density, and shape in such beds are essentially unlimited, but fundamental insight into the general behaviour of such systems can be gained by studying systems containing two types of particles[64 - 68]. When such materials are fluidized, mixing and segregation of particles appear to depend on particle density and particle size distribution and gas flow rate[69]. Experimental determination of the minimum fluidizing velocity is complicated in these systems. The normal procedure to determine U_{mf} by gradually decreasing superficial gas velocity is no longer satisfactory because well-mixed (homogeneous) conditions within the bed cannot be attained at velocities near U_{mf}. Correlations for estimating the minimum fluidization velocity of binary systems have been proposed by various investigators and some of them are reviewed and compared by Chyang et al.[68].

Two different approaches have been employed for estimating the minimum fluidization velocity of mixtures of different particle sizes. The first approach is to develop an empirical correlation directly from experimental values of U_{mf} (refs[65,68]):

$$U_{mf}^{mix} = U_s (U_b/U_s)^{x_b^2}, \qquad (60)$$

where U_{mf}^{mix} denotes the minimum fluidizing velocity of a mixture of particles of sizes b and s, U_b and U_s are the respective minimum fluidizing velocities of the bigger and smaller particles and x_b is the weight fraction of bigger particles.

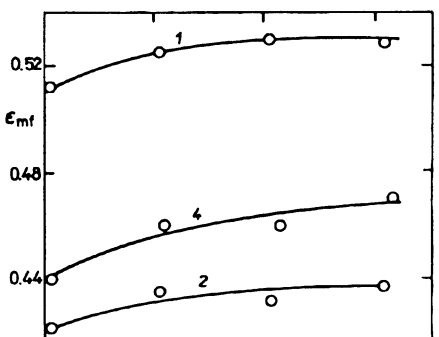

FIG. 8

Influence of pressure on the bed voidage at minimum fluidization: carbon particles, ρ_s = 850 kg m^{-3} (ref.[62]): $\bar{d}_p$: *1* 0.066 mm, *2* 0.108 mm, *3* 0.171 mm; coal particles, ρ_s = 1 247 kg m^{-3} (ref.[34]): *4* $\bar{d}_p$ = 0.358 mm

The second approach involves introducing an effective particle diameter and an effective density concepts into those expressions which have been developed for monodisperse systems. Several formulae for calculating such effective parameters have been proposed, but agreement among them is not good and widely different values of effective diameter and effective density can be obtained for a given mixture of particles.

The transition of a packed bed of polydisperse particles to a fluidized state takes place over a certain range of gas velocity[63,70,71]. The gas velocity at which small and/or light particles commence to fluidize is called the beginning fluidization velocity, U_{bf}. As gas velocity is increased further, a state of total fluidization can be attained. The gas velocity at which this occurs is designated the complete fluidization velocity, U_{cf}. It should be pointed out that, because of the range ($U_{bf} - U_{cf}$) of velocities during the onset of fluidization of a mixture, concept of a minimum fluidizing velocity, U_{mf}, at which fluidization of monodisperse particles begins, has little physical meaning for polydisperse materials as illustrated in Fig. 9. Although the value of U_{mf} indicated can be defined by the intersection of the two extrapolated lines, its physical interpretation is not precisely defined in terms of an observable phenomenon as is the case for a bed of monodisperse particles.

The dependences of three characteristic gas velocities on pressure as determined by an experimental procedure of slow defluidization of a polydisperse system are shown in Fig. 10. The complete fluidization velocity, U_{cf}, is most strongly influenced by

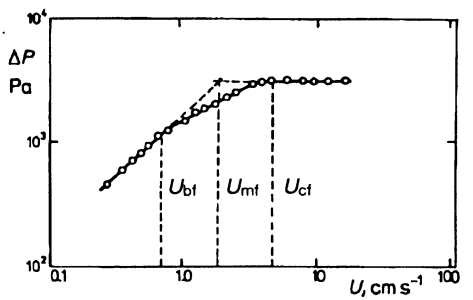

FIG. 9
Pressure drop vs superficial gas velocity for a polydisperse bed of coal particles. Mean particle size, $\bar{d}_p$ = 0.138 mm (size range: 0.09 – 0.36 mm); ρ_s = 1 262 kg m^{-3}; fluidized with nitrogen[63]

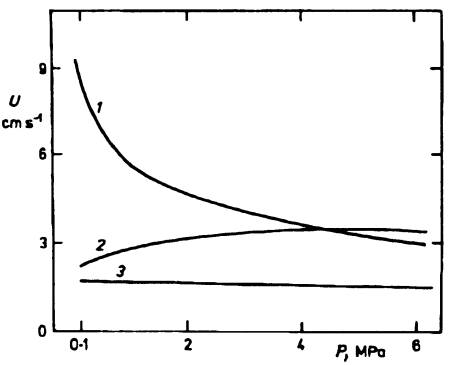

FIG. 10
Effect of pressure on the different states of a polydisperse bed of coal particles: *1* velocity at which fluidization is complete, *2* velocity at which bubbling begins, *3* velocity at which fluidization begins. Mean particle size, $\bar{d}_p$ = 0.181 mm (size range: 0.09 – 0.38 mm); fluidized with nitrogen[63]

pressure. Although U_{cf} decreases rapidly with pressure, the minimum bubbling velocity increases weakly as pressure increases. This behaviour of U_{mb} is in accord with the common observation that the fluidization is easier and smoother when carried out under elevated pressure.

The complete fluidization velocity is defined as the velocity at which all particles are fully engaged or supported by the gas even though segregation by size can occur. Knowlton[72] proposed the predictive equation

$$U_{cf} = \sum x_i U_{mfi}, \qquad (61)$$

where U_{mfi} and x_i refer to the i-th sieve fraction of size d_{pi} and the summation is taken over all size fractions.

5. CONCLUSIONS

The validity of the Ergun equation is generally recognized. This predictive relationship has a firm theoretical foundation and is well-supported by experimental data, particularly for uniform spheres of nearly spherical particles.

The physical picture is not that clear in cases of non-spherical particles which are commonly used in practice. Shape factor and the bed voidage at incipient fluidization are useful theoretical concepts that can be measured or estimated only imperfectly in concrete systems. The bed voidage is not a well-defined function of the particle shape. Moreover, it is a well-established fact that the minimum fluidization velocity is very sensitive to variations in bed voidage. Quantitative descriptions of fluidization also suffer from the complexity of defining and measuring unambiguously such fundamental parameters as the size and size distribution of a mixture of particles. Considering these difficulties, it is not surprising that the predictive relationships provide estimates of U_{mf} with accuracy not better than ±30%. The generalized, empirical equations of Wen and Yu[31], Broadhurst and Becker[6] and Lucas et al.[35] are practically equivalent in this regard and the accuracy of their predictions lies within generally accepted limits. The reliability of all assumed and measured parameters that can influence the behaviour of fluidized beds should always be carefully considered. A decision whether to employ a predictive equation or to resort to experimental measurements of the minimum fluidization velocity must rest on a rational assesment of such reliability. Experiments certainly are necessary in cases of irregularly shaped or nonspherical particles, or materials exhibiting wide ranges of sizes.

SYMBOLS

a	parameter given by Eq. (*14*)
b	parameter given by Eq. (*15*)
A	shape-voidage function given by Eq. (*21*)

Ar	$= d_p^3\, g\ \rho_f(\rho_s - \rho_f)/\mu_f^2$, Archimedes number
B	shape-voidage function given by Eq. (*22*)
C	parameter in Eq. (*16*)
C_D	drag coefficient of sphere
C_1	parameter in Eq. (*35*)
C_2	parameter in Eq. (*35*)
d_p	mean sieve size of solids, m
$\bar{d}_p$	mean particle size given by Eq. (*6*), m
d_{pi}	arithmetic mean of adjacent sieve apertures, m
d_{pm}	median corresponding to the 50% value on the cumulative curve, m
d_{sv}	diameter of a sphere having the same surface/volume ratio as the particle, m
d_v	diameter of a sphere having the same volume as the particle, m
$f(\varepsilon)$	porosity function
F	cross-sectional area of empty vessel, m^2
g	= 9.807 m s^{-2}, acceleration due to gravity
H	height of bed, m
H_{mf}	height of bed at the minimum fluidization point, m
H_0	height of fixed bed, m
k_1, k_2	coefficients in Eq. (*53*)
M	molecular weight, kg $kmol^{-1}$
M_p	mass of a single particle, kg
n	parameter in Eq. (*16*)
P	pressure in Eqs (*43*), (*44*), kPa
ΔP	pressure drop across a bed, Pa
Re	$= U\, d_p\, \rho_f/\mu_f$, Reynolds number
Re_{mf}	$= U_{mf}\, d_p\, \rho_f/\mu_f$, Reynolds number at the point of minimum fluidization
Re_t	$= U_t\, d_p\, \rho_f/\mu_f$, Reynolds number at terminal free-fall velocity
t	temperature, °C
T	temperature, K
U	superficial fluid velocity, m s^{-1}
U_b	minimum fluidization velocity of bigger particles, m s^{-1}
U_{bf}	fluid velocity at beginning fluidization of polydisperse system, m s^{-1}
U_{cf}	fluid velocity at complete fluidization of polydisperse system, m s^{-1}
U_{mb}	minimum bubbling velocity, m s^{-1}
U_{mf}	minimum fluidization velocity, m s^{-1}
U_{mf}^{mix}	minimum fluidization velocity of a binary mixture, m s^{-1}
U_s	minimum fluidization velocity of smaller particles, m s^{-1}
U_t	terminal free-fall velocity, m s^{-1}
V_p	volume of a particle, m^3
W	mass of particles, kg
x_b	weight fraction of bigger particles
x_i	weight fraction of particles of a given size
Y	$= (\Delta P/H)\,(d_p^2/(\mu_f U))\,\varepsilon^3/(1-\varepsilon)^2$, quantity plotted in Fig. 1
δ	deviation from the mean value, %
ε	bed voidage (void fraction or porosity of bed)
ε_{mf}	bed voidage at the point of minimum fluidization
ε_0	bed voidage of fixed bed
μ_f	fluid viscosity, kg m^{-1} s^{-1}

μ_g	gas viscosity, kg m^{-1} s^{-1}
ρ_f	fluid density, kg m^{-3}
ρ_g	gas density, kg m^{-3}
ρ_{He}	skeletal (helium) density, kg m^{-3}
ρ_s	particle density, kg m^{-3}
σ	spread or standard deviation of particle size, m
Ψ	sphericity of particle, shape factor

The author (M. H.) gratefully acknowledges that his contribution to this work was supported in part by the Grant Agency of Academy of Sciences of the Czech Republic, grant No. 47208.

REFERENCES

1. Hartman M., Havlín V., Svoboda K., Kozan A. P.: Chem. Eng. Sci. *44*, 2770 (1989).
2. Hartman M., Svoboda K. in: *Encyclopedia of Fluid Mechanics* (N. P. Cheremisinoff, Ed.), Vol. 4, p. 757. Gulf Publ. Co., Houston 1986.
3. Yates J. G.: *Fundamentals of Fluidized-Bed Chemical Processes*, p. 4. Butterworths, London 1983.
4. Levenspiel O.: *Engineering Flow and Heat Exchange*, p. 135. Plenum Press, New York 1984.
5. Geldart D.: *Gas Fluidization Technology*, p. 11. Wiley, Chichester 1986.
6. Broadhurst T. E., Becker H. A.: AIChE J. *21*, 238 (1975).
7. Abrahamsen A. R., Geldart D.: Powder Technol. *26*, 35 (1980).
8. Knight M. J., Rowe P. N.: Chem. Eng. Sci. *35*, 997 (1980).
9. Leva M.: Chem. Eng. Prog. *43*, 549 (1947).
10. Brownell L. E., Dombrowski H. S., Dickey C. A.: Chem. Eng. Prog. *46*, 415 (1950).
11. Kozeny J.: Ber. Wien. Akad. *136a*, 271 (1927).
12. Carman P. C.: Trans. Inst. Chem. Eng. *15*, 150 (1937).
13. Burke S. P., Plummer W. B.: Ind. Eng. Chem. *20*, 1196 (1928).
14. Ergun S.: Chem. Eng. Prog. *48*, 89 (1952).
15. Macdonald I. F., El-Sayed M. S., Mow K., Dullien F. A. L.: Ind. Eng. Chem., Fundam. *18*, 199 (1979).
16. Dullien F. A. L.: Chem. Eng. J. *10*, 1 (1975).
17. Nakamura M., Hamada Y., Toyama S.: Can. J. Chem. Eng. *63*, 8 (1985).
18. Svoboda K., Čermák J., Hartman M., Drahoš J., Selucký K.: Ind. Eng. Chem., Process Des. Dev. *22*, 514 (1983).
19. Svoboda K., Čermák J., Hartman M., Drahoš J., Selucký K.: AIChE J. *30*, 513 (1984).
20. Fan L. T., Huang Y. W., Yutani N.: Chem. Eng. Sci. *41*, 189 (1986).
21. Shi Y.-F., Yu Y. S., Fan L. T.: Ind. Eng. Chem., Fundam. *23*, 484 (1984).
22. Biswal K. C., Samal B. B., Roy G. K.: J. Inst. Eng. (India) *65*, 15 (1984).
23. Biswal K. C., Bhowmik T., Roy G. K.: Chem. Eng. J. *30*, 57 (1985).
24. Wen C. Y., Yu Y. H.: Chem. Eng. Prog., Symp. Ser. *62*, 101 (1966).
25. Kmiec A.: Chem. Eng. J. *11*, 237 (1976).
26. Kmiec A.: Chem. Eng. J. *23*, 133 (1982).
27. Khan A. R., Richardson J. F.: Chem. Eng. Sci. *45*, 255 (1990).
28. Hartman M., Havlín V., Trnka O., Čársky M.: Chem. Eng. Sci. *44*, 1743 (1989).
29. Hartman M., Veselý V., Svoboda K., Havlín V.: Collect. Czech. Chem. Commun. *55*, 409 (1990).
30. Schiller L., Neumann A.: Z. Ver. Deutsch. Ing. *77*, 318 (1933).
31. Wen C. Y., Yu Y. H.: AIChE J. *12*, 610 (1966).

32. Saxena S. C., Vogel G. J.: Trans. Inst. Chem. Eng. *55*, 184 (1977).
33. Grace J. R. in: *Handbook of Multiphase Systems* (G. Hetsroni, Ed.), p. 8-1. Hemisphere Corp., Washington, D. C. 1982.
34. Chitester D. C., Kornosky R. M., Fan L.-S., Danko J. P.: Chem. Eng. Sci. *39*, 253 (1984).
35. Lucas A., Arnaidos J., Casal J., Puigjaner L.: Ind. Eng. Chem., Process Des. Dev. *25*, 426 (1986).
36. Lucas A.: Ind. Eng. Chem. Res. *26*, 182 (1987).
37. Kocurek J., Hartman M.: Int. Chem. Eng. *31*, 715 (1991).
38. Svoboda K., Hartman M.: Ind. Eng. Chem., Process Des. Dev. *20*, 319 (1981).
39. Goroshko V. D., Rozenbaum P. B., Todes D. M.: Izv. Vyssh. Ucheb. Zaved., Neft Gaz *1*, 125 (1958).
40. Svoboda K., Hartman M.: AIChE J. *27*, 866 (1981).
41. Hartman M., Svoboda K.: Ind. Eng. Chem., Process Des. Dev. *26*, 649 (1986).
42. Pattipati R. R., Wen C. Y.: Ind. Eng. Chem.; Process Des. Dev. *20*, 705 (1981).
43. Botterill J. S. M., Teoman Y., Yüregir K. R.: Powder Technol. *31*, 101 (1982).
44. Flamant G., Fatah N., Steinmetz D., Murachman B., Laguerie C.: Int. Chem. Eng. *31*, 673 (1991).
45. Desai A., Kikukawa H., Pulsifier A.: Powder Technol. *16*, 143 (1977).
46. Doheim M. A., Collinge C. N.: Powder Technol. *21*, 284 (1978).
47. Botterill J. S. M., Teoman Y., Yüregir K. R.: Chem. Eng. Commun. *15*, 227 (1982).
48. Stubington J. F., Barreth D., Lowry G.: Chem. Eng. Sci. *39*, 1516 (1984).
49. Rowe P. N.: Chem. Eng. Sci. *40*, 2003 (1985).
50. Bin A. K.: Chem. Eng. Sci. *40*, 2004 (1985).
51. Yang W.-Ch., Chitester D. C., Kornosky R. M., Keairns D. L.: AIChE J. *31*, 1086 (1985).
52. Shristawa S., Mathur A., Saxena S. C.: AIChE J. *32*, 1227 (1986).
53. Yamazaki R., Veda N., Jimbo G.: J. Chem. Eng. Jpn. *19*, 251 (1986).
54. Lucas A., Arnaldos J., Casal J., Puigjaner L.: Chem. Eng. Commun. *41*, 121 (1986).
55. Saxena S. C., Mathur A., Zhang Z. F.: AIChE J. *33*, 500 (1987).
56. Hartman M., Veselý V., Svoboda K.: Collect. Czech. Chem. Commun. *56*, 822 (1991).
57. Pata J., Čársky M., Hartman M., Veselý V.: Ind. Eng. Chem. Res. *27*, 1493 (1988).
58. Rowe P. N.: Chem. Eng. Sci. *39*, 173 (1984).
59. Hoffmann A. C., Yates J. G.: Chem. Eng. Commun. *41*, 133 (1986).
60. Chan I. H., Sishtla C., Knowlton T. M.: Powder Technol *53*, 217 (1987).
61. Olowson P. A., Almstedt A. E.: Chem. Eng. Sci. *45*, 1733 (1990).
62. Weimer A. W., Quarderer G. J.: AIChE J. *31*, 1019 (1985).
63. Sciazko M., Bandrowski J.: Chem. Eng. Sci. *40*, 1861 (1985).
64. Chiba S. T., Chiba T., Nienow A. W., Kobayashi H.: Powder Technol. *22*, 255 (1979).
65. Cheung L., Nienow A. W., Rowe P. N.: Chem. Eng. Sci. *29*, 1301 (1974).
66. Uchida S., Yamada H., Tada I.: J. Chin. Inst. Chem. Eng. *14*, 257 (1983).
67. Vaid R. P., Sen Gupta P.: Can. J. Chem. Eng. *56*, 292 (1978).
68. Chyang Ch.-S., Kuo Ch.-Ch., Chen M.-Y.: Can. J. Chem. Eng. *67*, 344 (1989).
69. Čársky M., Veselý V., Pata J.: Collect. Czech. Chem. Commun. *51*, 1618 (1986).
70. Kumar A., Sen Gupta P.: Indian J. Technol. *12*, 225 (1974).
71. Obata E., Watanabe H., Endo N.: J. Chem. Eng. Jpn. *15*, 23 (1982).
72. Knowlton T. M.: Presented at *67th Annual Meeting of AIChE, Washington, D.C., 1974*, Paper No. 7.6.

Translated by the author (M. H.).